Recurrent neural networks model based reliability assessment of power semiconductors in PMSG converter

Liu, Shiyi; Zhou, Dao; Wu, Chao; Blaabjerg, Frede

Published in:
Microelectronics Reliability

DOI (link to publication from Publisher):
10.1016/j.microrel.2021.114314

Publication date:
2021

Document Version
Publisher's PDF, also known as Version of record

Microelectronics Reliability 126 (2021) 114314

Contents lists available at ScienceDirect

Microelectronics Reliability

journal homepage: www.elsevier.com/locate/microrel

Recurrent neural networks model based reliability assessment of power semiconductors in PMSG converter

Shiyi Liu *, Dao Zhou, Chao Wu, Frede Blaabjerg

Department of Energy Technology, Aalborg University, Aalborg, Denmark

ARTICLE INFO

Keywords:
Recurrent neural networks
Power semiconductors
Loss and thermal models
Reliability analysis

ABSTRACT

To obtain accurate lifetime evaluation with acceptable simulation time for fulfilling the total life cycle design criteria, this paper proposes a Recurrent Neural Networks (RNN) based model with the replacement of the Simulink model. It starts with the establishment of the Averaged Switch (AS) model and Averaged Fundamental (AF) model of the Permanent Magnet Synchronous Generators (PMSG) to calculate accumulated damage. Then, under the same mission profile, the junction temperature, rainflow counting and accumulated damage of the AS and AF model are calculated and compared. It can be noted that the AS model is more accurate to calculate the reliability of components, since both the big thermal cycles caused by load variations and the small thermal cycles due to the fundamental AC current are considered. However, it consumes more time compared to the AF model. To this end, the RNN model is proposed to substitute the most time consuming part of the system reliability evaluation procedure. With aid of proposed model, the consumed time can be greatly reduced compared with the Simulink model. In the end, a 1-hour case study is applied to verify the efficiency of the RNN model. The Mean Absolute Percentage Error (MAPE) of the testing case is 0.51% and the time for getting results in the RNN model is less than 1 s. Besides, an annual case is also implemented to verify the RNN model, which has an averaged 0.78% MAPE for the whole year.

1. Introduction

With increasing global renewable energy installation, the reliability analysis of the wind power system is gaining more attention. In Relia-Wind study [1], it is noted that the power converter causes close to 30% of the total unexpected failures of an onshore wind turbine, and the power devices of power electronic system are the bottleneck of reliability assessment [2,3]. Inspired from this, more and more researchers focus on the reliability assessment for such active components (i.e. IGBT, diode, etc.) [2,4].

As mentioned in [4], the thermal cycles with various amplitudes in the active power components can be the failure reason in the wind turbine system. However, the thermal cycles of the power semiconductors can be divided into two types [5]. One kind is the big thermal cycles, resulting from the loading fluctuation, such as varying loading currents and ambient temperatures, which are ranged from seconds to years. The other kind is known as the small thermal cycles, based on fundamental frequency of the loading current, ranging from milliseconds to seconds, which is caused by the conduction and switching from the freewheeling diodes to the IGBTs during a fundamental period of the Alternating Current (AC) in the generator and the power grid [6].

For evaluating the reliability of the active components, the detailed lifetime calculation process is described in [7]. The detailed model of power loss and thermal simulation are used to obtain the dynamic thermal stress, including both the small and big cycles. Since it is built with the small time steps, the affordable simulation time of this model is restricted due to the calculation burden, which indicates that it is hard to be used to estimate the lifetime consumption with one-year mission profile.

To solve this problem, the existing methods to calculate the lifetime is mainly based on [6], where only steady-state condition is considered with compromised accuracy of big thermal dynamics. The small thermal cycles are regarded as constants with the annual wind speed distribution [8] or ignored [9]. And the big thermal cycles are obtained from mission profile by using the averaged fundamental model, which is introduced in [9] for obtaining the details below fundamental cycle. However, most of these approaches still need complicated calculation and analysis process to obtain the one-year lifetime consumption. In order to simplify the

* Corresponding author.
E-mail address: shli@et.aau.dk (S. Liu).

https://doi.org/10.1016/j.microrel.2021.114314
Received 27 May 2021; Received in revised form 19 June 2021; Accepted 20 July 2021
Available online 11 October 2021

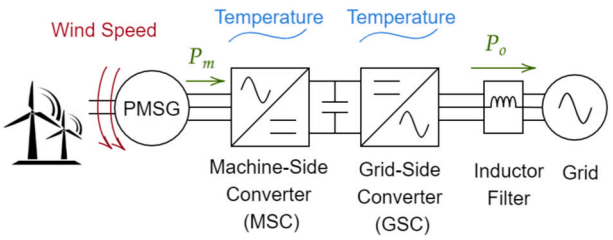

Fig. 1. Typical wind turbine configuration equipped with a PMSG.

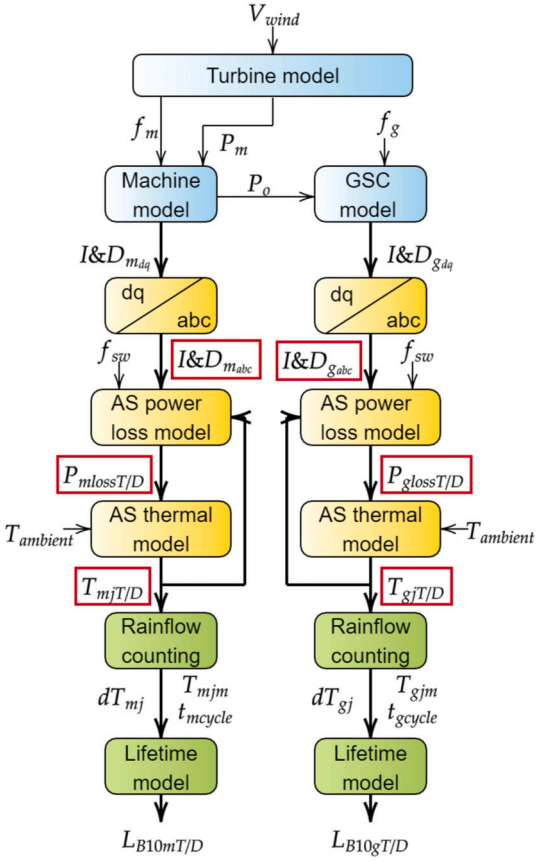

Fig. 2. Flow-chart to calculate damage of the power switches in MSC and GSC by using the Averaged Switch (AS) model.

relationship from mission profile to the junction temperature, [10] applies the look-up table to substitute the model. Nevertheless, as a data mapping method, it relies on huge amount of data and is only effective with the specific power converter. To overcome this disadvantage, an Artificial Neural Network (ANN) based model is proposed to substitute the power loss and thermal model in the process of reliability evaluation to simplify the calculation [11]. However, the estimation procedure in this literature is based on fixed ambient temperature and steady-state thermal cycling of the power semiconductor.

The idea behind the paper is to substitute the turbine model, machine and converter model, power loss model and thermal model of the system reliability evaluation procedure with an artificial intelligence based method that serves fast and accurate approximations of these steps. The novel aspects are summarized as follows: 1) Build and compare the Averaged Switch (AS) model and the Averaged Fundamental (AF) model; 2) Propose the Recurrent Neural Networks (RNN) based model to replace the key steps for reliability evaluation to obtain fast and accurate outcomes.

The structure of the paper is as follows: Section 2 introduces the reliability assessment of the individual components in the grid-side converter (GSC) and the machine-side converter (MSC) with the AS model and the AF model. Then the rainflow counting results and the accumulated damage from these two models are obtained and compared. Sections 3 proposes an RNN based model for the reliability assessment of power devices and benchmarks the thermal profile from the AS and AF models. An annual mission profile is illustrated in Section 4 and concluding statements are reached in Section 5.

Table 1
Parameter specification of wind turbine system.

Rated output power	2 MW
Grid frequency	50 Hz
DC-link voltage	1050 V
Rated amplitude of phase voltage	563 V
Cut-in wind speed	3 m/s
Cut-off wind speed	25 m/s
Number of pole pairs	102
Operational range of turbine speed	6-18 rpm
Rated rotor flux linkage	2.23 Wb
Stator inductance	0.28 mH
Line filter inductance	0.15 mH
Rated RMS current of GSC	1496 A
Rated RMS current of MSC	2085 A
Switching frequency	2 kHz
Stator current frequency	10.2-30.6 Hz

2. Reliability evaluation of power semiconductor in PMSG

The typical configuration of a Permanent Magnet Synchronous Generators (PMSG) is shown in Fig. 1. The stator winding of the generator is connected to the grid via the full-scale power converter, which contains an MSC and a GSC. Furthermore, the inductor filter is used to suppress the high-order harmonics [12].

In principle, the reliability evaluation of power semiconductors in the PMSG can be evaluated with two different models depending on the mission profile resolution.

2.1. Averaged switch model

In order to compare the AS and AF model, by using the same one-hour mission profile, the accumulated damage of power semiconductors in the GSC and MSC of the PMSG need to be obtained and evaluated. The structure to calculate the hourly accumulated damage of the power component in the converters of PMSG by using the AS model is shown in Fig. 2. The working conditions of the PMSG are specified in Table 1. Paralleled structure of 1 kA/1.7 kV half-bridge IGBT power modules are used to increase the current capability.

According to the Maximum Power Point Tracking (MPPT) together with turbine parameters given in Table 1, the relationship between the wind speed and the output power of the turbine P_m can be calculated. By neglecting the power losses of the PMSG, DC-link and the MSC, the active power flows through the MSC and the GSC are considered to be the same [13], which means that P_o is equal to P_m.

Then, combined with the machine and the GSC models, the average current flowing through the device $I_{m/g(dq)}$ and duty ratio of the IGBT or diode $D_{(m/g)(dq)}$ under dq axis can be obtained [14], where subscripts g and m denote the GSC and the MSC, subscripts d and q denote the d-axis and the q-axis. For obtaining the power loss, the inverse Park transformation is implemented to obtain the value of current $I_{m/g(abc)}$ and duty ratio $D_{m/g(abc)}$ under abc-axis, subscripts a, b and c denote the a-axis, the b-axis and the c-axis. After that, in accordance with the AS loss model and switching frequency f_{sw}, the AS power loss $P_{(m/g)loss(T/D)}$, which is composed of the switching and conduction loss of the IGBT and the diode in the GSC and the MSC, is deduced, where T and D denote the IGBT and diode. Their junction temperature $T_{(m/g)j(T/D)}$ can be obtained from the thermal model. The specific calculation process of the thermal

Table 2
Parameters of loss model and thermal model for power semiconductors [16,17].

	Symbol @ conditions	IGBT	Diode
Loss model	V_{ce} @ 1 kA T_j=125 °C (V)	2.31	/
	V_{ce} @ 1 kA T_j=25 °C (V)	1.86	/
	V_f @ 1 kA T_j=125 °C (V)	/	1.79
	V_f @ 1 kA T_j=25 °C (V)	/	1.71
	E_{on} @ 1 kA T_j=125 °C (mJ)	435.14	/
	E_{on} @ 1 kA T_j=25 °C (mJ)	292.71	/
	E_{off} @ 1 kA T_j=125 °C (mJ)	356.00	/
	E_{off} @ 1 kA T_j=25 °C (mJ)	243.29	/
	E_{rr} @ 1 kA T_j=125 °C (mJ)	/	149.00
	E_{rr} @ 1 kA T_j=25 °C (mJ)	/	109.00
Thermal model		4.5	6.3
	Fourth-order thermal resistance (from junction to case) R (K/kW)	18	21
		7.5	14.7
		0	0
		0.006	0.004
	Fourth-order thermal time constant (from junction to case) τ (s)	0.06	0.04
		0.5	0.2
		1	1
	Thermal grease thermal resistance R (K/kW)	16	17
	Hestsink thermal resistance R (K/kW)	60	
	Hestsink thermal time constant τ (s)	420	

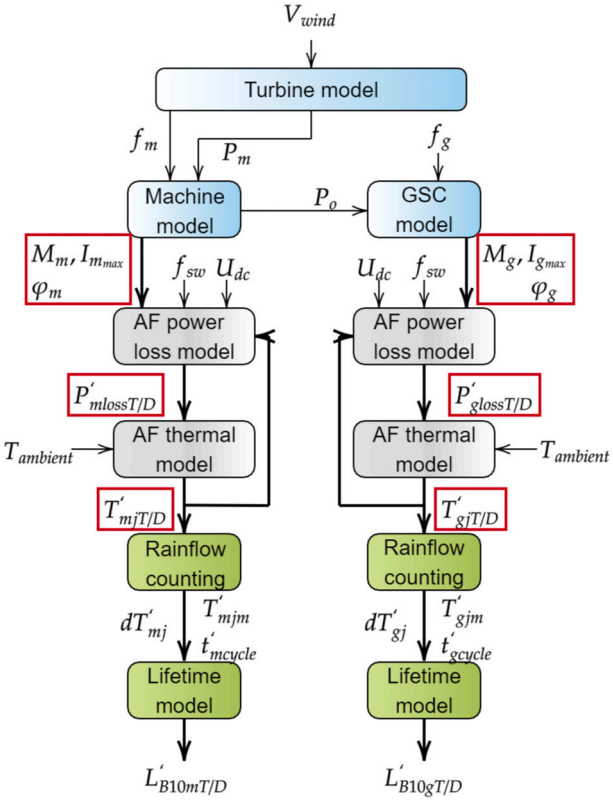

Fig. 3. Flow-chart to calculate damage of the power switches in MSC and GSC under Averaged Fundamental (AF) model.

model and power loss model are given in [15]. In addition, the parameters of the power loss model and thermal model are listed in Table 2.

For the lifetime assessment, the rainflow counting is implemented to derive the fluctuation $dT_{(m/g)j}$, mean value $T_{(m/g)jm}$ and the cycle period $t_{(m/g)cycle}$ of the thermal cycles. Finally, the lifetime model presented in [18] can be applied to estimate the lifetime $L_{B10(m/g)(T/D)}$ for the diode and IGBT in the GSC and the MSC by using the AS model.

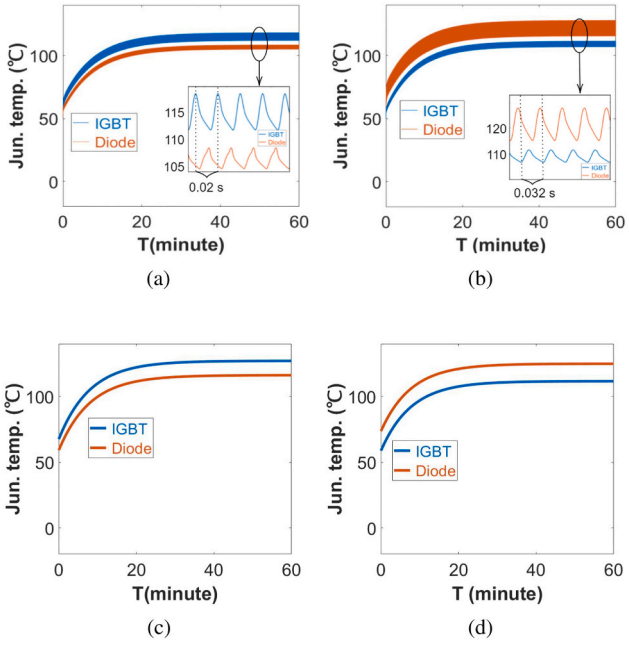

Fig. 4. Junction temperature results of diode and IGBT (a) In GSC from the AS model (b) In MSC from the AS model (c) In GSC from the AF model (d) In MSC from the AF model.

2.2. Averaged fundamental model

The structure to calculate the hourly accumulated damage of the power component in the GSC and the MSC by using the AF model is presented in Fig. 3. The working condition for wind turbine system, structure of converters and parameters of thermal and power loss model are the same as the AS model.

Compared to the AS model, the turbine model, machine model and GSC model are identical to the AS model. But the output is different from the AS model. The modulation index $M_{m/g}$, amplitude of converter phase current $I_{(m/g)\max}$, and the phase angle of the current with respect to voltage $\varphi_{m/g}$ can be calculated with the help from the machine and GSC model. After that, the calculation process of the power loss $P_{(m/g)loss(T/D)}{}'$, which has a constant profile within a fundamental period, and thermal temperature $T_{(m/g)j(T/D)}{}'$ of diode and IGBT in the AF model are given in [19]. Then with the new junction temperature for the diode and IGBT in the GSC and the MSC, the rainflow counting and lifetime model are applied to obtain the fluctuation $dT_{(m/g)j}{}'$, mean value $T_{(m/g)jm}{}'$ and the cycle period $t_{(m/g)cycle}{}'$ of the new thermal cycles and the new lifetime $L_{B10(m/g)(T/D)}{}'$. The lifetime model is basically identical with it in the AS model.

2.3. Comparison between the AS model and the AF model

In order to assess and compare the hourly accumulated damage of the component in the GSC and MSC of the PMSG by using the AS model and the AF model, the worst ambient temperature (50 °C) is applied. The wind speed is assumed at 12 m/s during this 1 h to reach the rated output power. The resolution of mission profile is set as 500e-6 s.

As shown in Fig. 4, the junction temperature profiles for the diode and the IGBT in the MSC and GSC from the AS contain both the big thermal cycles and the fundamental frequency based thermal cycles (i.e, the frequency is 50 Hz for the GSC and the frequency is 30.6 Hz for the MSC). Moreover, with the influence from the time constant of the thermal model, the fluctuation and mean value of the junction temperature is varying before they reach the steady-state. However, in the AF model, the junction temperature profiles only contain the big thermal cycles, which are caused by the heatsink thermal time constant before

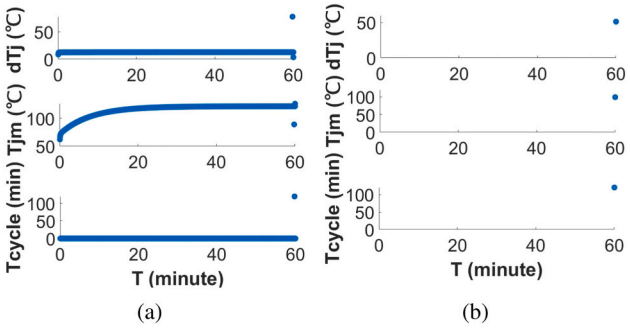

Fig. 5. Rainflow counting results of diode in GSC (a) from AS model (b) from AF model.

Table 3
Comparison between the AS and AF model.

		AF model	AS model
Mission profile resolution (s)		0.12	500e-6
Simulation step (s)		0.12	500e-6
Total simulation time (minute)		60	60
Total time consuming (minute)		5	45
Accumulated damage	Diode in MSC	2.05e-4	3.48e-4
	Diode in GSC	6.20e-5	7.60e-5
	IGBT in MSC	5.83e-5	2.83e-4
	IGBT in GSC	1.04e-4	2.12e-4

the steady-state.

With the significantly different junction temperature curves from the AS model and the AF model, the corresponding rainflow counting results demonstrate a huge difference. For instance, the rainflow counting results of the diode in the MSC from the AS model and AF model are shown in Fig. 5 as an example. As the cycles from the AS model contain both the small fundamental-frequency cycles and the big constant cycles, the rainflow counting results are composed by a lot of points. While in Fig. 5 (b), there is only one point due to the fact that the AF model only considers the big thermal cycles. It is evident that the accumulated damage of the AS model is much higher than the value from the AF model. The comparison between the AS model and the AF model under this case is shown in Table 3. It can be seen that the hourly accumulated damage of the diode/IGBT in the GSC/MSC from the AS model is always higher than the value from the AF model. It is noted that the result from the AF model is not accurate enough for estimating the damage of the wind turbine system. Hence, the AF model is used for the steady-state operation, whose impact from the simulation step can be ignored. However, the AS model is very detailed model with limited time span [7]. It can be used to obtain the lifetime containing both long and short-thermal dynamics.

3. Proposed recurrent neural networks based modeling

As summarized in the previous section, the AS model can provide results with both big thermal cycles and small thermal cycles. However, the process for getting the temperature profiles of the IGBT and diode in GSC and MSC in the AS model, which is built in Simulink, takes around 45 min for the hourly mission profile with 500e-6 s sample rate. Hence, there are some researches focusing on the simplified model. In [11], an ANN based model is used to substitute the power loss and thermal model in the process of reliability evaluation, with the fixed ambient temperature and steady-state operation. However, as illustrated in Figs. 2 and 3, the output of the power loss model and thermal model is always decided by the pervious thermal state in both the AF model and the AS model, which means that the output should be time-series. Besides, the variation of conduction state and thermal dynamics are not considered during the steady-state. Therefore, it is essential to establish a simple

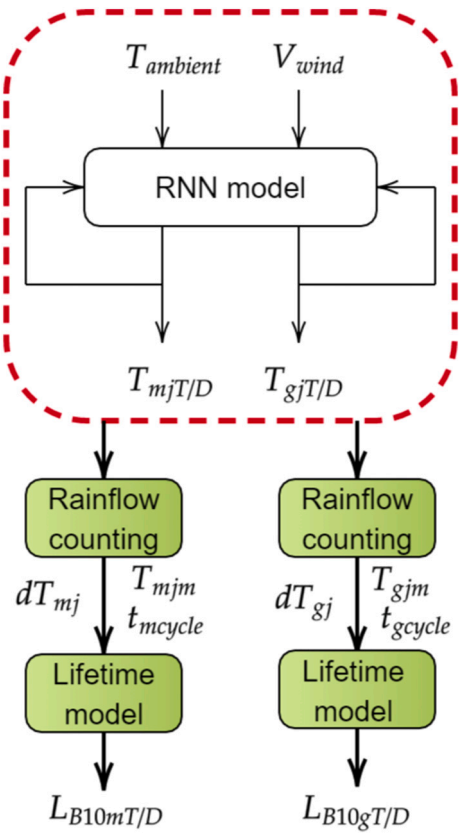

Fig. 6. Flow-chart to calculate damage of the power switches in MSC and GSC using RNN model.

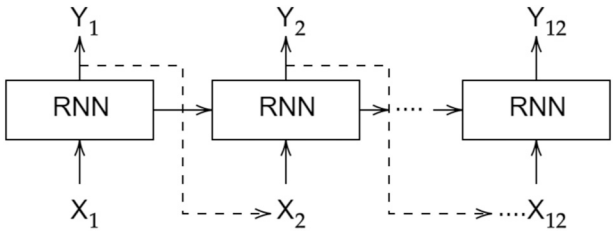

Fig. 7. Recurrent Neural Networks Based model.

model of the converter that is able to translate the time-series mission profile data into a time-series junction temperature.

Under this condition, the Recurrent Neural Networks (RNN) based model is proposed to simplify the process. The structure of using RNN model to calculate the accumulated damage is showed in Fig. 6. The RNN based model is introduced to substitute the calculation process from mission profile to the junction temperature, including the turbine model, machine model, GSC model, power loss model and thermal model. The junction temperature $T_{(m/g)j(T/D)}$ can be obtained from the RNN model. Then same as the other two models, the rainflow counting is applied and the lifetime will be evaluated.

RNNs are a type of neural networks that take into account historical information of a time series to enable future predictions [20]. In this case, because the power loss is affected by the junction temperature, another layer is added to produce the output y for each point and use it as a part of input for next moment. Fig. 7 shows the architecture of an RNN composed by 12 RNN units, which is every hour result, sampled every 5 min. It is noted that the impact of sample rate can be ignored [21]. In this paper, since the wind speed data is sampled every 5 min, the same sample rate is applied.

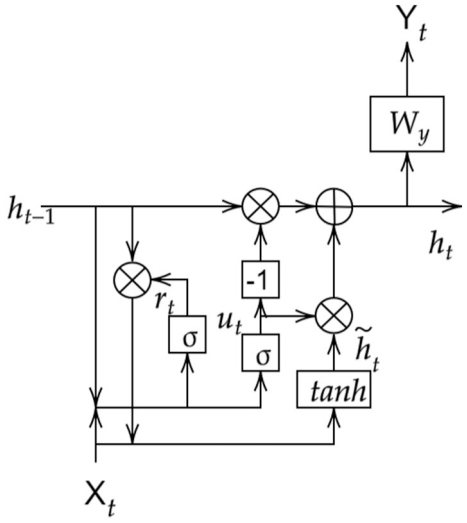

Fig. 8. Information flowing inside RNN unit.

The information flowing inside the RNN unit is illustrated as Fig. 8 and the specific computations are shown as follows.

$$r_t = \sigma(W_r x_t + U_r h_{t-1}) \tag{1}$$

$$u_t = \sigma(W_u x_t + U_u h_{t-1}) \tag{2}$$

$$\widehat{h}_t = (W_h x_t + U_h(r_t \odot h_{t-1})) \tag{3}$$

$$h_t = u_t \odot h_{t-1} + (1 - u_t) \odot \widehat{h}_t \tag{4}$$

$$y_t = \phi(W_y h_t) \tag{5}$$

where h_{t-1}, $h_t \in \mathbb{R}^{C'}$ are hidden states, $\odot$ denotes the element-wise multiplication, weight matrices W_r, W_u, W_h,$W_y \in \mathbb{R}^{C' \times C}$, U_r, U_u, $U_h \in \mathbb{R}^{C \times C}$, $\sigma(\cdot)$ is the sigmoid function, and $\phi(\cdot)$ is a non-linear activation function, e.g., *tanh*.

An RNN uses a reset gate r_t, represented in Eq. (1), to choose how much information should be discarded from the previous timestamp. A similar gate u_t, called update gate, is calculated using Eq. (2). Both the reset and update gates decide how much information from the history need to be considered for future predictions. Specifically, the RNN computes an internal state $\widehat{h}_t$ that takes as input x_t and h_{t-1}, and applies the reset gate r_t, as shown in Eq. (3).

In Eq. (4), the RNN utilizes the update gate u_t to merge the internal state $\widehat{h}_t$ and the hidden state h_{t-1} from the previous state, and the hidden state h_t is output. By doing this, the RNN remembers historical hidden states that are relevant to future predictions and forgets those that are irrelevant. In Eq. (5), the RNN output the current state $\widehat{y}_t$ which will be used as a part of input for x_{t+1}.

Hence, in this case, X_t is composed by $V_{wind(t)}$, $T_{ambient(t)}$, $T_{gj(t-1)}$, $T_{gd(t-1)}$, $T_{mj(t-1)}$, $T_{md(t-1)}$. The Y_t is composed by $T_{gj(t)}$, $T_{gd(t)}$, $T_{mj(t)}$, $T_{md(t)}$. Finally, the input for this model is hourly wind speed and ambient temperature, while the output is temperature of the IGBT and the diode in the back-back converters.

For assessing the accuracy of the RNN based model, the Mean Absolute Percentage Error (MAPE) is calculated, defined as Eq. (6).

$$MAPE = \frac{\sum_{t-1}^{n} \frac{|a_t - f_t|}{|a_t|}}{n} \tag{6}$$

where a_t is the value from the original model, f_t denotes the value from the RNN based model.

To verify and compare the RNN based model with the AS model, the same mission profile as shown in Fig. 4 is applied, and the junction profiles are presented in Fig. 9. it can be seen that the results from the RNN model is very close to the AS model, and the time for obtaining this result is less than 1 s compared to 45 min in the AS model. Furthermore, the MAPE of this case is 0.51%.

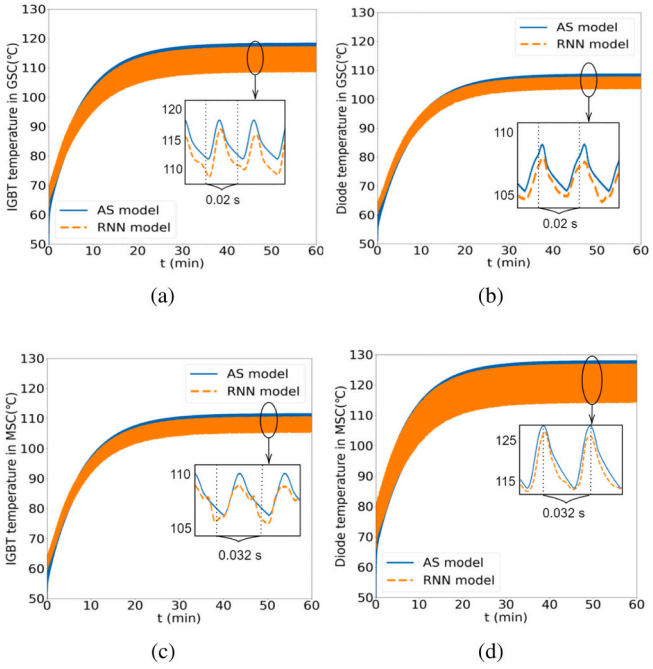

Fig. 9. Junction temperature results of diode and IGBT from the AS model and RNN model. (a) IGBT in GSC. (b) Diode in GSC. (c) IGBT in MSC. (d) Diode in MSC.

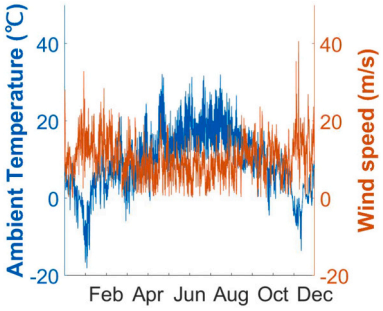

Fig. 10. Annual mission profile of one year in Aalborg.

4. Case study

In order to verify the proposed model, a case study for a 2 MW PMSG system has been carried out. As aforementioned in Section 2, the specification of the turbine and converter parameters of power loss model and thermal model are defined. Ambient temperature and wind speed data sampled every 5 min for a whole year are available from Aalborg/Denmark, as shown in Fig. 10.

Based on the mission profile, the whole year temperature curves of the IGBT and the diode in back-back converters can be obtained using the AS model in Simulink. This dataset was then randomly divided into three datasets, i.e., the training set (60% of data, corresponding to 7 months' data), the validation set (20% of data, corresponding to 2.5 months' data), and the testing set (20% of data, corresponding to 2.5 months' data). It should be noted that the amount of data may affect the final precision, but the impact from data division ratio can be ignored

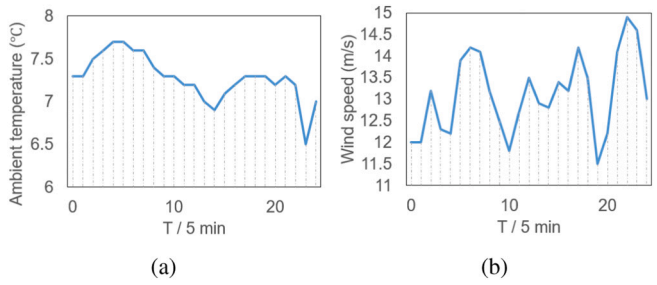

Fig. 11. The mission profile for testing the accomplished RNN model (a) ambient temperature (b) wind speed.

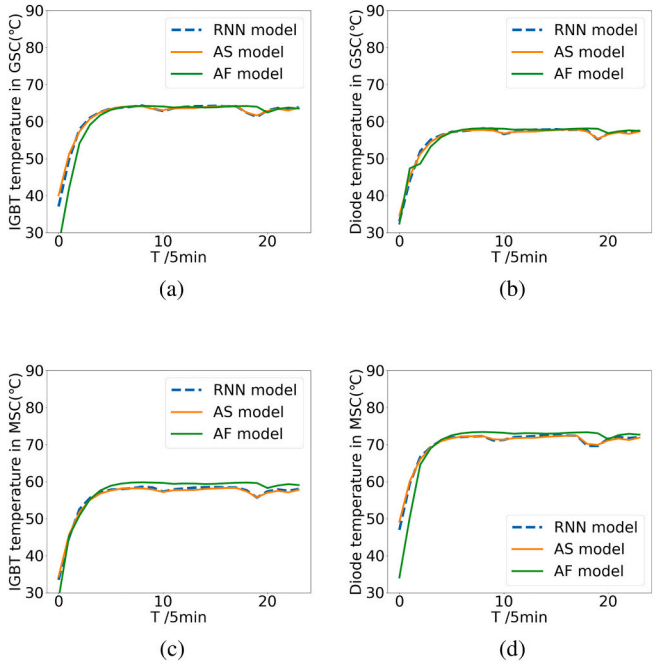

Fig. 12. Temperature of the IGBT and the diode in the GSC and MSC for 2 h under different model. (a) IGBT in GSC. (b) diode in GSC. (c) IGBT in MSC. (d) diode in MSC.

[22]. The averaged MAPE of this dataset is 0.78% in average, which is calculated based on the whole year profiles (considering all the seasons and every cases during this year). Due to the way of calculating the MAPE, as shown in Eq. (6), the biggest MAPE show up when the junction temperature is very close to 0, which is 2.15%. Theoretically, after the accomplished training phase, with any input of ambient temperature and wind speed, the RNN model is able to calculate the corresponding temperature.

To present the accuracy and efficiency of the RNN based model, a two-hour mission profile with the maximum ambient temperature and maximum wind speed curves are applied. Then the value from RNN model and the AS model in Simulink can be assessed and compared under the same random mission profile with 5 min sample rate.

The mission profiles for this case study can be seen in Fig. 11. The ambient temperature is around 10C and the wind speed is from 12 to 15 m/s. Fig. 12 shows the comparison of results from Simulink model and RNN model, sampled every 5 min. The MAPE under this condition is 0.67%, and the time for getting results in RNN model is less than 1 s. But in Simulink, it takes around 45 min to obtain 1-hour results.

5. Conclusion

In this paper, an artificial intelligence aided method to simplify the process of obtaining the chip temperature has been proposed. An averaged switch model of the GSC and MSC to calculate accumulated damage including the long and short-thermal dynamics is established and compared with an averaged fundamental model. It can be noted that the AS model serves to better calculate the reliability of components to fulfill the total life cycle design criteria, but it consumes more time than the AF model. Based on this situation, an RNN model is proposed to substitute the time consuming steps of the system reliability evaluation procedure, which serves faster and accurate approximations. With the aid of proposed model, the MAPE is 0.51% with the 1-hour extreme mission profile and 0.78% in average with the annual dataset of Aalborg. In the end, to show the accuracy and efficiency of the RNN model, a two-hour mission profiles is applied to assess and compare the results from the RNN model and the Simulink model. The MAPE under this condition is 0.67% and the time for getting 1-hour results in RNN model is less than 1 s compared with 45 min by using the simulation.

CRediT authorship contribution statement

Shiyi Liu: Conceptualization, Methodology, Software, Data curation, Writing- Original draft preparation and Visualization.
Dao Zhou: Supervision, Writing, Reviewing and Editing.
Chao Wu: Supervision, Writing, Reviewing and Editing,
Frede Blaabjerg: Supervision.

Declaration of competing interest

The authors declare that they have no known competing financial interests or personal relationships that could have appeared to influence the work reported in this paper.

Acknowledgements

The authors would like to thank Razvan Gabriel Cirstea for his help in setting up the RNN model of the power electronic system as shown in Fig. 7.

References

[1] L.M. Moore, H.N. Post, Five years of operating experience at a large, utility-scale photovoltaic generating plant, Prog. Photovolt. Res. Appl. 16 (3) (2008) 249–259.
[2] M. Liserre, R. Cárdenas, M. Molinas, J. Rodriguez, Overview of multi-mw wind turbines and wind parks, IEEE Trans. Ind. Electron. 58 (4) (2011) 1081–1095.
[3] S. Yang, A. Bryant, P. Mawby, D. Xiang, L. Ran, P. Tavner, An industry-based survey of reliability in power electronic converters, IEEE Trans. Ind. Appl. 47 (3) (2011) 1441–1451.
[4] G. Zhang, D. Zhou, J. Yang, F. Blaabjerg, Fundamental-frequency and load-varying thermal cycles effects on lifetime estimation of dfig power converter, Microelectron. Reliab. 76 (2017) 549–555.
[5] K. Ma, M. Liserre, F. Blaabjerg, Lifetime estimation for the power semiconductors considering mission profiles in wind power converter, in: 2013 IEEE Energy Conversion Congress and Exposition, 2013, pp. 2962–2971.
[6] D. Zhou, F. Blaabjerg, Converter-level reliability of wind turbine with low sample rate mission profile, IEEE Trans. Ind. Appl. 56 (3) (2020) 2938–2944.
[7] K. Ma, F. Blaabjerg, Multi-timescale modelling for the loading behaviours of power electronics converter, in: 2015 IEEE Energy Conversion Congress and Exposition (ECCE), IEEE, 2015, pp. 5749–5756.
[8] D. Zhou, F. Blaabjerg, T. Franke, M. Tonnes, M. Lau, Comparison of wind power converter reliability with low-speed and medium-speed permanent-magnet synchronous generators, IEEE Trans. Ind. Electron. 62 (10) (2015) 6575–6584.
[9] I. Vernica, H. Wang, F. Blaabjerg, Impact of long-term mission profile sampling rate on the reliability evaluation of power electronics in photovoltaic applications, in: 2018 IEEE Energy Conversion Congress and Exposition (ECCE), 2018, pp. 4078–4085.
[10] A. Sangwongwanich, Y. Yang, D. Sera, F. Blaabjerg, Lifetime evaluation of grid-connected pv inverters considering panel degradation rates and installation sites, IEEE Trans. Power Electron. 33 (2) (2018) 1225–1236.
[11] T. Dragicevic, P. Wheeler, F. Blaabjerg, Artificial intelligence aided automated design for reliability of power electronic systems, IEEE Trans. Power Electron. 34 (8) (2019) 7161–7171.
[12] H. Alaboudy, A. Daoud, S. Desouky, A. Salem, Converter controls and flicker study of pmsg-based grid connected wind turbines, Ain Shams Eng. J. 4 (1) (2013) 75–91.

[13] H. Zhang, L.M. Tolbert, Efficiency impact of silicon carbide power electronics for modern wind turbine full scale frequency converter, IEEE Trans. Ind. Electron. 58 (1) (2011) 21–28.
[14] H. Zhang, L.M. Tolbert, Sic's potential impact on the design of wind generation system, in: 2008 34th Annual Conference of IEEE Industrial Electronics, 2008, pp. 2231–2235.
[15] M. Musallam, C. Yin, C. Bailey, M. Johnson, Mission profile-based reliability design and real-time life consumption estimation in power electronics, IEEE Trans. Power Electron. 30 (5) (2015) 2601–2613.
[16] SEMIKRON, Datasheet for IGBT Module SKM1000GB17R8, 2020.
[17] L. Wei, R.J. Kerkman, R.A. Lukaszewski, Evaluation of power semiconductors power cycling capabilities for adjustable speed drive, in: 2008 IEEE Industry Applications Society Annual Meeting, 2008, pp. 1–10.
[18] Application Note AN2010-02, Infineon, Germany, Technical Information IGBT Modules Use of Power Cycling Curves for IGBT 4, 2012.
[19] D. Zhou, G. Zhang, F. Blaabjerg, Optimal selection of power converter in dfig wind turbine with enhanced system-level reliability, IEEE Trans. Ind. Appl. 54 (4) (2018) 3637–3644.
[20] I. Goodfellow, Y. Bengio, A. Courville, Deep Learning vol. 1, MIT press, Cambridge, 2016.
[21] D. Neil, M. Pfeiffer, S. Liu, Phased lstm: Accelerating Recurrent Network Training for Long or Event-based Sequences, 2016 arXiv preprint arXiv:1610.09513.
[22] J. Chung, C. Gulcehre, K. Cho, Y. Bengio, Empirical Evaluation of Gated Recurrent Neural Networks on Sequence Modeling, 2014 arXiv preprint arXiv:1412.3555.